

## SEISMIC RESPONSE OF A REINFORCED CONCRETE ARCH BRIDGE

Kazuhiko KAWASHIMA<sup>1</sup> And Atsushi MIZOGUTI<sup>2</sup>

### SUMMARY

This paper presents an analysis of the seismic response characteristics and seismic performance of an arch bridge, which was designed in accordance with the traditional static design approach based on the allowable stress design method, under a strong ground motion recorded in the 1995 Hyogo-ken nanbu, Japan, earthquake. Nonlinear dynamic response analysis was conducted considering the uniform excitation and multiple excitation. It was found from the analysis that the vertical excitation is very important, and hence should be considered in design. It was also found that large axial force, which is about two times the design axial force, and even tension force are developed in the arch rib as well as the flexural yielding.

### INTRODUCTION

The 1995 Hyogo-ken nanbu, Japan, earthquake revealed the fact that a certain type of bridges which are designed without moderate seismic consideration based only on the traditional elastic design approach are vulnerable to seismic disturbance. Although arch bridges have not yet suffered damage in the past including the 1994 Northridge earthquake and the 1995 Hyogo-ken nanbu earthquake, this does not give credit to be safe in an extreme earthquake since they were located far from the epicenters. Since arch bridges are generally constructed at stable rock site, they have not yet experienced strong seismic disturbance. Because the arch rib is designed so that it is mainly subjected to axial force, and because the variation of axial force is induced associated with the lateral force, it is a major concern that how large flexural moment and variation of axial force are induced in the arch rib.

Seismic performance of arch bridges has been clarified by many researchers in recent years. For example, Kuranishi and Nakajima [1986] studied the dynamic strength of deck-type steel arch bridge subjected to axial excitation. Dusseau and Wen [1989], Nazmy and Konidaris [1994] and Sakakibara et al [1998] also analyzed the nonlinear behavior of steel arch bridges. Sakakibara et al reported that significant flexural yielding occurred in a steel arch bridge subjected to the Kobe type ground motion. This paper presents a series of nonlinear dynamic response analyses on the seismic response characteristics and the seismic performance of a reinforced concrete arch bridge subjected to a strong ground shaking developed in the 1995 Hyogo-ken nanbu earthquake.

### ARCH BRIDGE AND ANALYTICAL IDEALIZATION

#### Arch Bridge Analyzed

Fig. 1 shows an arch bridge analyzed. It is a highway bridge with two lanes (9.5 m wide), and has a center span

length of 150 m and an arch rise of 27 m. Since the arch span vs. rise ratio is 1/5.6, it is a standard configuration as an arch bridge. Both ends of the deck are supported by steel movable bearings in longitudinal direction. The arch rib and the deck were connected together at the arch crown. The vertical members are rigidly connected to the arch ribs and pin-connected to the deck. Seismic design was originally conducted in accordance with the

<sup>1</sup> Department of Civil Engineering, Tokyo Institute of Technology, Tokyo, Japan Email: kawasima@cv.titech.ac.jp

<sup>2</sup> Department of Civil Engineering, Tokyo Institute of Technology, Tokyo, Japan Email: kawasima@cv.titech.ac.jp

1980 Design Specifications of Highway Bridges [Japan Road Association, 1980] based on the allowable stress design approach. The seismic coefficient of 0.18 was assumed in both longitudinal and transverse directions.

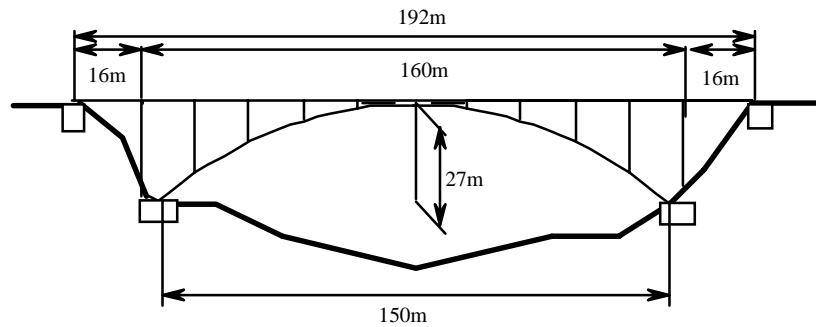


Figure 1: Bridge analyzed

Fig. 2 shows the sections of arch rib at springing. It is of box sections. At both springings, 60 deformed bars with 22 mm diameter (D22) are placed 150 mm spacing along both inner and outer face of upper and lower flanges. Also 22 D22 bars are placed 150 mm spacing along both faces of the webs. Thus, the longitudinal reinforcement ratio is 1.0-1.5 %. D19 ties are placed 150 mm spacing. D 19 cross ties are also provided 150 mm spacing in the flanges and webs. However, both ties and cross ties are anchored by 90 degree hook in the covering concrete.

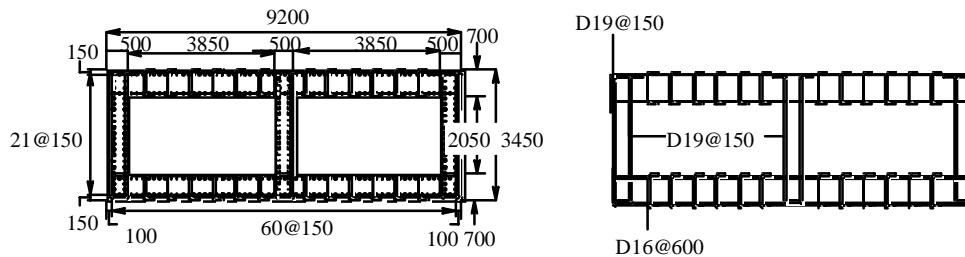


Figure 2: Section of arch rib and arch crown at springing

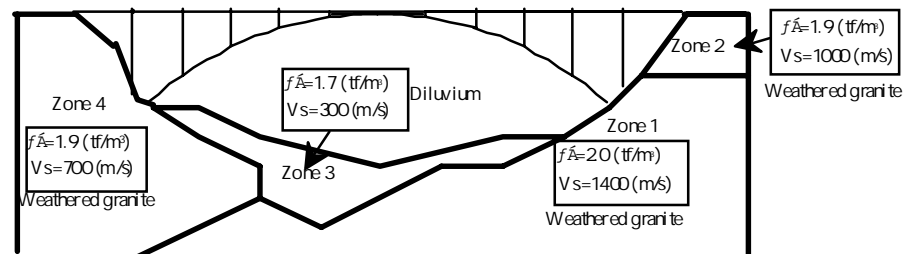


Figure 3: Ground condition

The ground around the bridge is of rock as shown in Fig. 3. The rock around the right abutment is weathered granite. Upper part is more weathered. Rock around the left abutment is more weathered than the right hand side. The valley is of sedimentation. Shear wave velocity of the right and left rock is approximately 1400 m/s and 700 m/s, respectively. Soil condition is Type I based on the classification of the Design Specifications of Highway Bridges.

### Analytical Idealization

The arch bridge was idealized as a discrete analytical model as shown in Fig. 4. The deck and the vertical members were idealized by the linear beam elements. Since large variation of axial force occurs in the arch rib, it is important to consider the nonlinear interaction of axial force and flexural moment. However since a reliable analytical model to take account of the large variation of axial force was not available, only flexural nonlinearity was considered in this analysis. Thus, the arch rib was idealized by flexural nonlinear beam elements with the Takeda type hysteretic behavior [Takeda et al, 1970]. The skeleton of the hysteretic model of the arch rib was assumed to be elsto-plastic with the yielding stiffness  $K_y$  and the yielding curvature  $\phi_y$  as;

$$K_y = \frac{M'_y}{\phi'_y}; \phi_y = \phi'_y \frac{M_y}{M'_y} \quad (1)$$

where,  $M'_y$ = initial yielding moment and  $\phi'_y$ = initial yielding curvature. Since the ties and cross ties in the arch rib are anchored in the covering concrete, they are not effective in confining the concrete when the covering concrete spalls off. Furthermore, evaluation of nonlinear behavior of hollow arch rib section subjected to large flexural moment under significant variation of axial force is difficult. Therefore as a first trial, the initial yielding moment and the initial yielding curvature were computed based on the standard moment vs. curvature analysis [Japan Road Association, 1996] assuming that all ties and cross ties are effective in confining the core concrete [Hoshikuma et al, 1997] and that the axial force does not vary from the initial value induced by the static load.

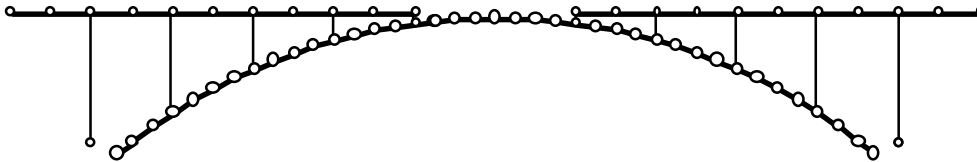


Figure 4: Analytical model

### Ground Motion and Idealization of Surrounding Ground

Acceleration recorded at the Kobe Observatory of the Japan Meteorological Agency in the Hyogo-ken nanbu earthquake was used as an input motion. The rock around the site was idealized by a two dimensional discrete model with the energy transmitting boundary at the both sides of the rock model. The base rock was assumed rigid. The computer program FLUSH [Lysmer et al, 1975] was used in the idealization. The NS and vertical components of the JMS Kobe Observatory record were prescribed at the height of right springing and they were deconvoluted to compute the base rock accelerations by SHAKE [Schnabel,et al, 1972]. The base rock accelerations were then applied to the two dimensional model to compute the ground motion at the right and left springings. The shear strain dependency of the equivalent stiffness and damping ratio of rocks was taken into account in analysis.

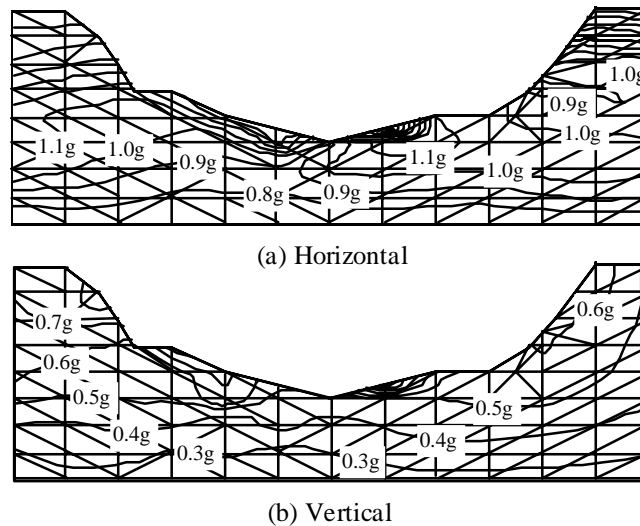
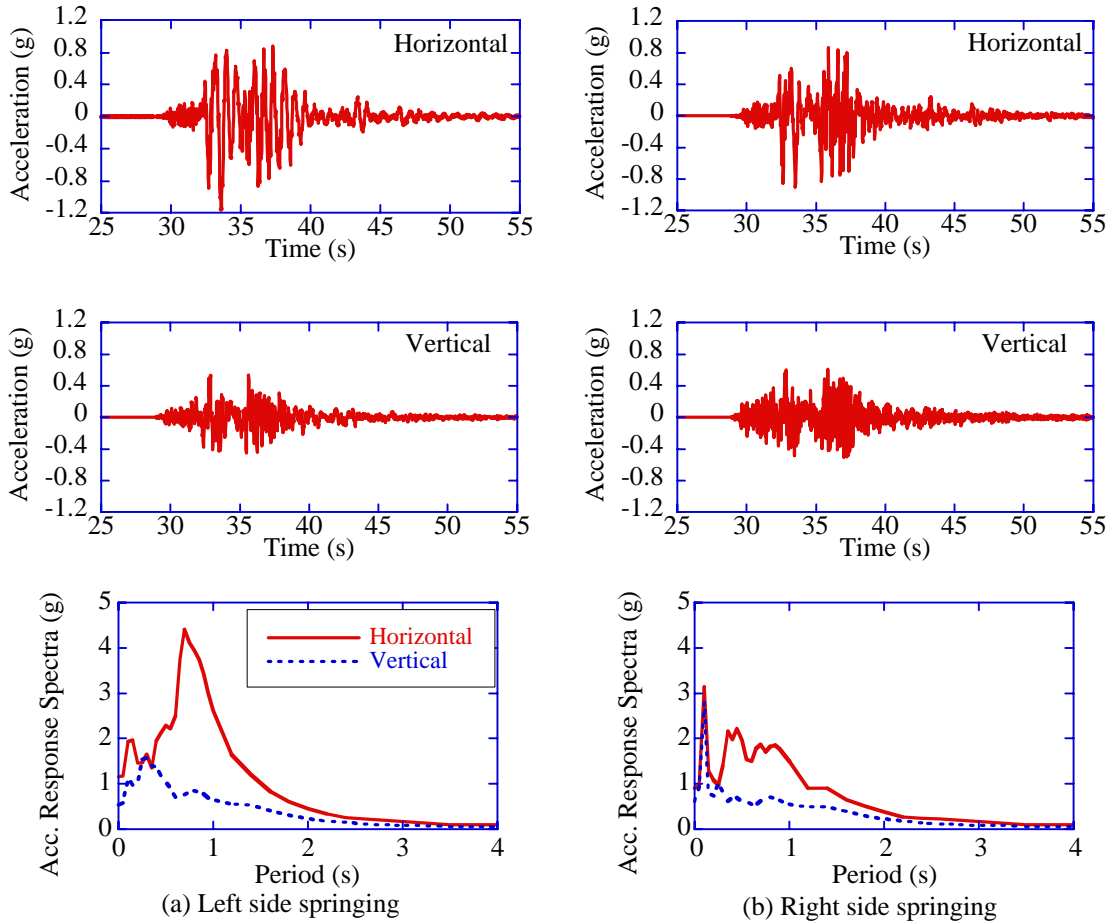


Figure 5: Response acceleration in surrounding ground

Fig. 5 shows the horizontal and vertical accelerations computed for the surrounding ground. Since the shear wave velocity of the rock in the left side is lower than that in the right side, the amplification of acceleration is higher in the left side. Fig. 6 shows the acceleration thus computed at the both springings as well as the acceleration response spectra with damping ratio of 0.05. The peak accelerations are 0.91 g (horizontal) and 0.61 g (vertical) at the right side and 1.15 g (horizontal) and 0.53 g (vertical) at the left side. They were used for the input motions for the arch bridge.



**Figure 6: Ground accelerations computed at both springings**

### Natural Periods and Natural Mode Shapes

Fig. 7 and Table 1 show the natural mode shapes, natural periods and mode participation factors for major modes. It is seen that 1st and 3rd are the anti-symmetric horizontal modes, while 2nd and 4th are the symmetrical vertical modes. It is also seen that the accumulated effective mass from 1st to 8th is only 46 % of the total mass. This implies that the higher modes are important to evaluate the response of the arch bridge.

**Table 1: Natural periods, mode participation factor and effective mass**

| Mode No. | Natural Period | Mode Participation Factor | Effective Mass | Percentage of Effective Mass Ratio |
|----------|----------------|---------------------------|----------------|------------------------------------|
| 1        | 2.00           | 13.63                     | 1.82           | 26                                 |
| 2        | 1.07           | 0                         | 0              | 26                                 |
| 3        | 0.612          | -4.68                     | 0.21           | 29                                 |
| 4        | 0.447          | 0                         | 0              | 29                                 |
| 5        | 0.338          | -10.7                     | 1.12           | 45                                 |
| 6        | 0.317          | 0                         | 0              | 45                                 |
| 7        | 0.234          | 0                         | 0              | 45                                 |
| 8        | 0.229          | 2.58                      | 0.65           | 46                                 |

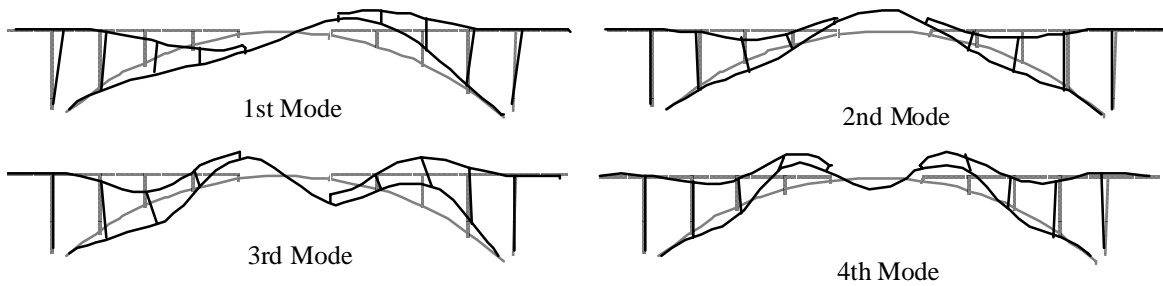


Figure 7: Natural mode shapes

### DEFORMATION TO STATIC LOADS

The axial force and the bending moment of the arch rib due to the static dead load is shown in Fig. 8. The axial force and the bending moment due to the load combinations of "dead load"+"active load," and "dead load"+"active load"+"thermal effect," which are the most predominant in design, are presented. The design axial force and the design bending moment thus determined and used in design are also presented in Fig. 8 for comparison.

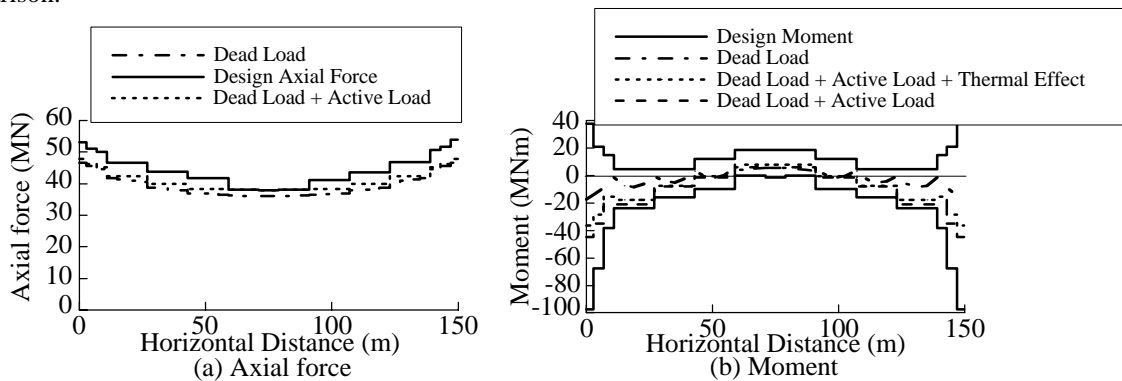


Figure 8: Axial force and bending moment due to static loads

It is seen in Fig. 8 that approximately 90 % of the axial force is induced by the dead load. Although it is not presented here, limited increase of the axial force occurs by applying the lateral seismic force equivalent to the 0.18 lateral force coefficient. Since the allowable stress can be increased 1.5 time for a load combination of the "dead load"+"seismic effect," none of the sections of the arch rib requires modification due to the seismic effect.

On the other hand, the bending moment induced by the dead load is only 20 % of the design value, and the rest is contributed by the active load and the thermal effect. However as is the axial force, no modification is required for the arch section by the seismic effect.

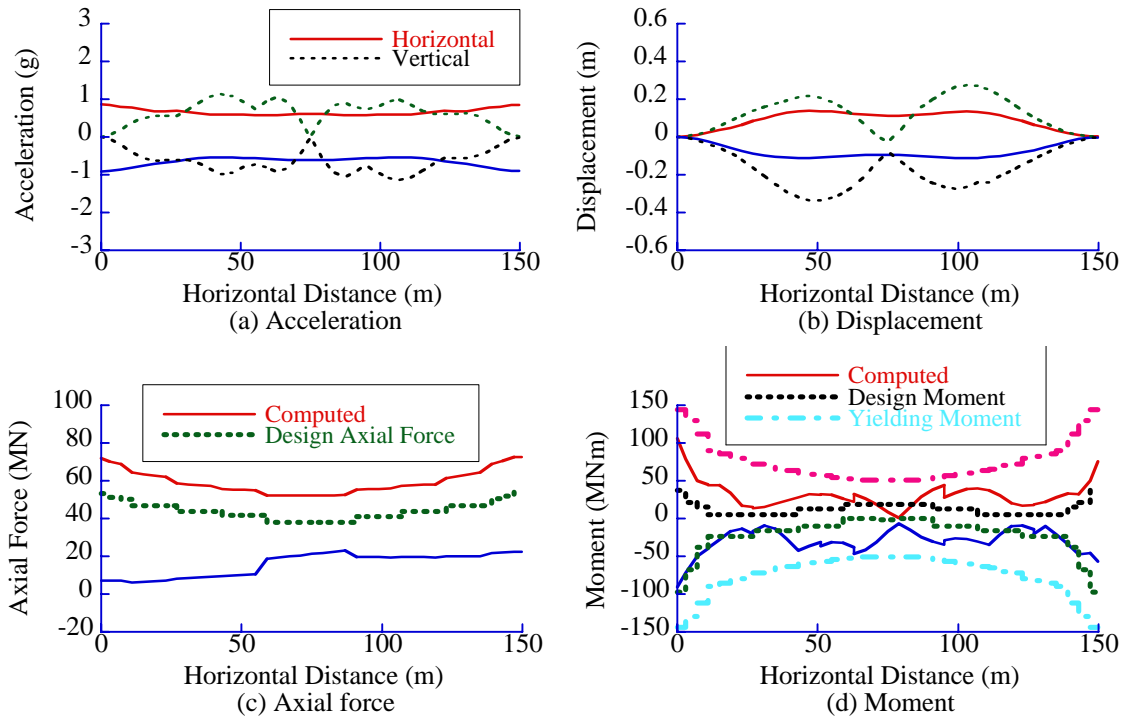
### SEISMIC RESPONSE SUBJECTED TO UNIFORM EXCITATION

To understand the basic response characteristics of the arch bridge, the response of the bridge subjected to only uniform horizontal ground motion was first analyzed. The horizontal acceleration at right side presented in Fig. 6(b) was applied as an input motion to the arch bridge at both springings.

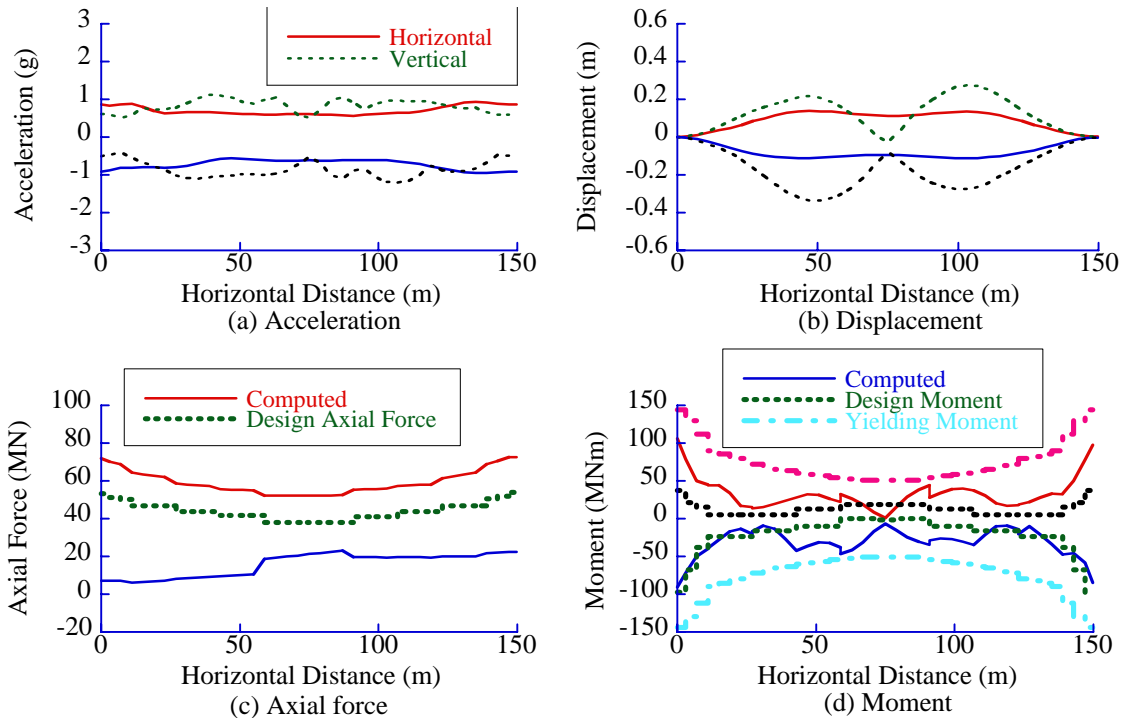
Fig. 9 (a) and (b) show the peak response acceleration and displacement in both lateral and vertical directions. The maximum lateral acceleration of 0.8 g occurs at both springings, while the maximum lateral displacement of 0.15 m occurs at the 1/4 and 3/4 points in the arch rib. It is noteworthy that over 1g acceleration and over 0.3 m displacement occur in the vertical direction in spite of the fact that the excitation is given only in horizontal direction. This is due to the significant mode coupling in the arch bridge between the horizontal and vertical direction as shown in Fig. 7.

Fig.9 (c) and (d) show the axial force and bending moment induced in the arch rib. The forces induced by the dead load are included in Fig. 9 (c) and (d). Effect of the horizontal excitation can be found by comparing Fig. 9

(c) and (d) to Fig. 8. It is seen that the axial force increases about 20 % by applying the horizontal excitation, and exceeds the design axial force. The bending moment induced by the horizontal excitation also exceeds the design moment at most points. Since it is smaller than the yielding bending moment, yielding does not occur. However it should be noted here that nonlinear interaction of axial force and bending moment is disregarded in this analysis. If the axial force of the arch rib decreases, the yielding moment of the arch rib decreases, thus it is possible that more significant yielding occurs in the arch rib. More careful and elaborated analysis is required for such effect.



**Figure 9: Peak acceleration, displacement, axial force and bending moment of arch rib when the bridge is subjected to only uniform lateral excitation**



**Figure 10: Peak acceleration, displacement, axial force and bending moment of arch rib when the bridge is subjected to uniform lateral and vertical excitations**

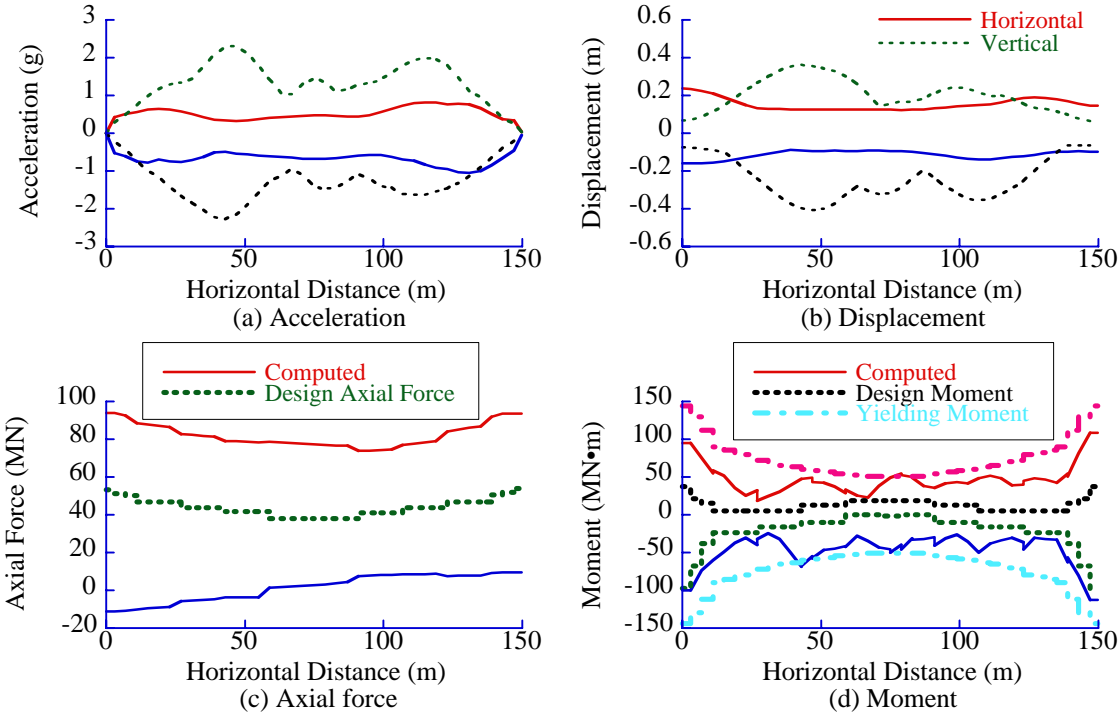
Next, the vertical ground motion in addition to the horizontal acceleration was applied to the arch bridge at both springings. The ground response at the right side (refer to Fig. 6(b)) were used for the ground motion. Fig. 10 (a) and (b) show the peak response acceleration and displacement of the arch rib. Although the increase of lateral responses associated with the vertical excitation is less significant, the vertical responses increase by adding the vertical excitation. The effect is more clearly observed in the axial force presented in Fig. 10 (c). At the left springing, the maximum axial force increased from 60 MN to 70 MN and the minimum axial force decreased from 20 MN to 10 MN by applying the vertical excitation. As shown in Fig. 10 (d), the bending moment also slightly increases by considering the vertical excitation. However since it is smaller than the yielding moment, the flexural yield does not occur in the arch rib.

**SEISMIC RESPONSE SUBJECTED TO MULTIPLE EXCITATION**

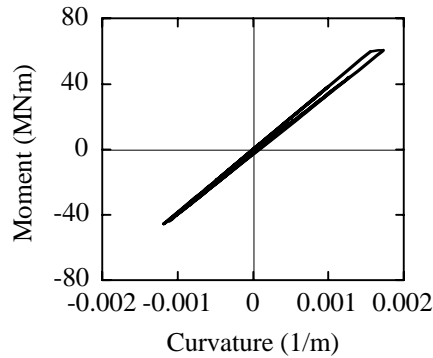
Fig. 11 (a) and (b) show the peak response acceleration and displacement when the arch bridge is subjected to the multiple excitation. The ground motions in horizontal and vertical directions computed at the right and left springings were applied to the arch bridge at the right and left springings, respectively, as the input motions. It should be noted here that direct comparison of the displacement response to the previous results cannot be made since the displacement presented in Fig. 11 (b) is the absolute displacement while the displacement presented in Figs. 9 (b) and 10 (b) are the relative displacement. The acceleration response, in particular in vertical direction, increases significantly by applying the multiple excitation. It is noteworthy to remind here that the ground motion at the left springing is larger than that at the right springing.

Fig. 11 (c) and (d) show the axial force and bending moment induced in the arch rib. The axial force significantly increases in the multiple excitation; the maximum axial force significantly exceeds the design value, and even tension force is induced. Although the tension is only 10 MN, 20 % of the design axial force, it is important in the evaluation of seismic performance of the arch bridge since no consideration has been paid that seismic force brings the tension in the arch rib. Furthermore, flexural yielding occurs at the rib where jointed rib and deck zone at the crown ends. Fig. 12 shows the moment vs. curvature relation at the rib where flexural yield occurs. Although curvature ductility factor is only 1.1, it should be noted that further larger nonlinearity may be developed if the nonlinear interaction be properly considered in the analysis.

It is important to note in the above results that tension force as well as some flexural yielding occurs in the arch rib designed in accordance with the traditional seismic coefficient method. More careful and elaborated analysis is required to evaluate the seismic performance.



**Figure 11: Peak acceleration, displacement, axial force and bending moment of arch rib when the bridge is subjected to multiple excitations**



**Figure 12: Moment vs. curvature relation at arch rib**

## CONCLUSION

A series of linear and nonlinear dynamic response analysis as well as the static and eigen value analyses were conducted to clarify the seismic response characteristics and the seismic performance of a reinforced concrete arch bridge designed in accordance with the traditional seismic coefficient method. The Kobe type ground motion was assumed as an input motion in the analysis. From the analysis presented herein, the following conclusions may be deduced:

1. In addition to the lateral response, large vertical response acceleration and displacement are induced by the lateral excitation due to significant mode coupling between lateral and vertical modes. The vertical excitation contributes to the axial force and bending moment in the arch rib. Thus, it is important to consider the vertical excitation in seismic design of an arch bridge.
2. Large compression force which is about double the design axial force and even some tension force are induced in the arch rib when subjected to the Kobe type ground motion. Furthermore, slight yield occurs in the arch rib.
3. The nonlinear interaction between axial force and flexural moment was disregarded in this analysis. Therefore it is anticipated that more significant yielding occurs in the arch rib when the nonlinear interaction is properly included in analysis. Although it was assumed here that hoops and cross ties are effective in confining the core concrete, this should be critically re-evaluated if the yielding occurs in the arch rib.

## REFERENCES

- Dusseau, R. A. and Wen, R. K. (1989), "Seismic Responses of Deck-Type Arch Bridges," *Earthquake Engineering and Structural Dynamics*, 18, pp701-715.
- Hoshikuma, J., Kawashima, K., Nagaya, K. and Taylor, A. W. (1997), "Stress-Strain Model for Confined Reinforced Concrete in Bridge Piers," *Journal of Structural Engineering*, ASCE, 123, 5, pp624-633.
- Japan Road Association (1980), "Part V Seismic Design, Design Specifications of Highway Bridges," Tokyo.
- Japan Road Association (1996), "Part V Seismic Design, Design Specifications of Highway Bridges," Tokyo.
- Kuranishi, S. and Nakajima, A. (1986), "Strength Characteristics of Steel Arch Bridges subjected to Longitudinal Acceleration," *Structural Engineering/ Earthquake Engineering*, Japan Society of Civil Engineers, 3, 2, pp287-296.
- Lysmer, J., Udaka, T., Tsai, C. F. and Seed (1975), "FLUSH - A Computer Program for Approximate 3 D Analysis of Soil-Structure Interaction Problems," Earthquake Engineering Research Center, University of California, Berkeley, Report No. EERC 75-30, CA, USA.
- Nazmy, A. S. and Konidaris, E. G. (1994), "Nonlinear Seismic Behavior of Steel Deck-Type Arch Bridges," 5th US National Conference on Earthquake Engineering, Chicago, Illinois, USA.
- Sakakibara, Y., Kawashima, K. and Shoji, G. (1998), "Analytical Evaluation of An Upper-Deck Type Two-Hinge Steel Arch Bridge," *Journal of Structural Engineering*, Japan Society of Civil Engineers, 44A, pp761-767.
- Schanabel, P. B., Lysmer, J. and Seed, H. B. (1972), "SHAKE - A Computer Program for Earthquake response Analysis of Horizontally Layered Sites," Earthquake Engineering Research Center, University of California, Berkeley, Report No. EERC 72-12, CA, USA.
- Takeda, T., Sozen, M. A. and Nielsen, N. N. (1970), "Reinforced concrete response to simulated earthquakes," *Proc. 3rd Japan Earthquake Symposium*, pp357-364, Tokyo.